Tunneling and delay time of cutoff Gaussian wave packets

Jorge Villavicencio,[1,*] Roberto Romo,[2,†] and Elmer Cruz[2,3,‡]
[1]*Instituto de Ciencia de Materiales de Madrid (CSIC), Cantoblanco, 28049 Madrid, Spain*
[2]*Facultad de Ciencias, Universidad Autónoma de Baja California, Apartado Postal 1880, 22800 Ensenada, Baja California, México*
[3]*Centro de Investigación Científica y de Educación Superior de Ensenada, Apartado Postal 2372, 22860 Ensenada, Baja California, México*
(Received 1 September 2006; revised manuscript received 25 November 2006; published 23 January 2007)

A formal analytic solution of the time-dependent Schrödinger equation is obtained for cutoff Gaussian wavepackets incident on finite range potentials of arbitrary shape. We derive closed analytical expressions for transmitted wavepackets with a small cutoff and the solutions are applied to investigate the dynamics of wavepacket tunneling. We showed that the analytic solutions satisfy a useful rescaling property that was applied to study and characterize the delay time in delta potential barriers.

DOI: 10.1103/PhysRevA.75.012111 PACS number(s): 03.65.Xp

I. INTRODUCTION

The scattering of wavepackets by one-dimensional potentials has been a quantum dynamical model of great importance [1–13]. In addition to its academic interest as a pedagogical tool in quantum mechanics textbooks, this simple model has allowed to explore and understand a number of interesting transport phenomena, such as delay times, Hartman effect [2], and the dynamics of wavepackets in semiconductor superlattices [7,8,11].

Although one finds a few recent works that use analytical solutions, the approach based on full numerical solutions is mostly employed in the literature. In general, the possibility of having analytical solutions in terms of known functions, not only provides more insight into the physics of the system, but they are also versatile and faster computational tools.

In this work we apply the *quantum shutter* approach to the problem of scattering of Gaussian wavepackets by arbitrary one-dimensional potentials, and explicit analytic solutions are obtained. The truncation of the initial wavepacket (i.e., the cutoff of its front tail by the shutter; see Fig. 1) is the unique difference with respect to the traditional extended wavepacket (EWP), usually treated numerically. We demonstrate the existence of a regime in which our cutoff wavepacket (CWP) can be used as an excellent approximation for the EWP, providing in this way a formal analytic solution for the latter. In the present work we also derive exact analytic solutions for the particular cases of free propagation, tunneling through a delta potential, and tunneling through a finite thin barrier. Moreover, these easy-to-use analytic solutions have interesting mathematical properties, in particular, a rescaling property that is exploited to study a large number of systems in a single calculation.

We also apply our formalism of CWP's to the case of a delta potential in order to analyze the *delay time*. The mentioned rescaling property is used to extend the range of the parameters to unexplored regions, which allows us to characterize from a dynamical point of view the main features of the delay time.

In Sec. II we present the derivation of the formal solution for CWP's. Section III deals with a discussion of the truncation effects, and the derivation of the exact analytical solutions for the free propagation, the delta potential, and thin barrier in the low-energy regime. In Sec. IV we apply our formalism in order to carry out a dynamical analysis of the delay time for a delta potential. Finally, in Sec. V we present the concluding remarks.

II. FORMAL SOLUTION FOR CUTOFF GAUSSIAN WAVEPACKETS

In this section we shall derive the formal solution for exploring the tunneling dynamics of Gaussian CWP's within the quantum shutter approach [14,15]. Our model deals with a time-dependent solution of Schrödinger's equation for a finite range potential $V(x)$ that vanishes outside the region $0 \leqslant x \leqslant L$, with a CWP initial condition,

$$\psi(x,t=0) = \begin{cases} Ae^{-(x-x_0)^2/4\sigma^2} e^{ik_0 x}, & -\infty < x \leqslant 0, \\ 0, & x > 0. \end{cases} \quad (1)$$

This setup consists of a Gaussian wave packet centered at $x=x_0$ with an effective width σ, impinging on the left potential edge at $x=0$, and $t=0$. Here we have defined k_0 as the

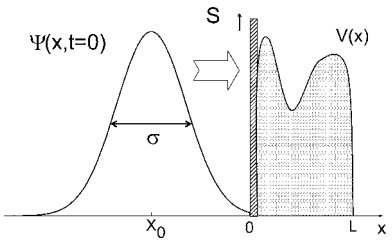

FIG. 1. Quantum shutter S for an initial cutoff Gaussian wavepacket with momentum k_0 centered at x_0, and effective width σ.

*Permanent address: Facultad de Ciencias, Universidad Autónoma de Baja California, Apartado Postal 1880, 22800 Ensenada, Baja California, México; electronic address: villavics@uabc.mx
†Electronic address: romo@uabc.mx
‡Also at Centro de Ciencias de la Materia Condensada, Universidad Nacional Autónoma de México, Apartado Postal 2681, 22835 Ensenada, Baja California, México.

initial momentum, where $E_0=(\hbar^2k_0^2/2m)$ is the incidence energy, and A is the corresponding normalization constant. While the EWP's are spread in the full spatial interval $(-\infty,+\infty)$, the CWP's, as mentioned above only exist in the semispace, $x<0$, at the initial time, $t=0$.

To obtain the time-dependent solution for $t>0$ along the transmission region $(x\geqslant L)$, we use the following expression [13,16]:

$$\psi(x,t)=\int_{-\infty}^{\infty}\frac{dk}{\sqrt{2\pi}}\phi(k)T(k)e^{ikx-i\hbar k^2t/2m}, \tag{2}$$

where $T(k)$ is the transmission amplitude of the problem and $\phi(k)$ is the Fourier transform of the initial cutoff state given by Eq. (1). The normalized expression for the latter reads,

$$\phi(k)=2\pi\Lambda_0 w(iz), \tag{3}$$

where we have defined a constant factor Λ_0 as,

$$\Lambda_0\equiv\frac{1}{2\pi}\sqrt{\frac{\sigma}{\sqrt{2\pi}}}\frac{1}{\sqrt{w(iz_0)}}, \tag{4}$$

which is related to the normalization constant A. In the above equations, $w(z)$ is the *complex error function* [17,18] defined as $w(z)=\exp(-z^2)\mathrm{erfc}(-iz)$, where $\mathrm{erfc}(z)$ is the complementary error function [17]; the arguments z and z_0 in Eqs. (3) and (4) are given by

$$z=\frac{x_0}{2\sigma}+i(k_0-k)\sigma,$$

$$z_0=\frac{ix_0}{\sqrt{2}\sigma}. \tag{5}$$

The time-dependent solution in x space along the transmission region is obtained by feeding Eq. (3) into Eq. (2). It reads

$$\psi(x,t)=\Lambda_0\int_{-\infty}^{\infty}dk\, w(iz)T(k)e^{ikx-i\hbar k^2t/2m}. \tag{6}$$

The above expression is the formal solution for Gaussian CWP's. It can be used to explore the space and time evolution of the system for a wide variety of potential profiles. The only relevant input is the transmission amplitude $T(k)$ associated to the arbitrary potential $V(x)$, defined along the interval $0\leqslant x\leqslant L$.

There are some interesting cases in which the evaluation of the solution (6) can be done analytically, which is one of the main advantages of using CWP's instead of EWP's. In the next section we shall discuss different cases of interest, and demonstrate the reliability of the CWP's solutions as approximations for EWP's in a special range of parameters.

III. PROBABILITY DENSITY: EFFECT OF TRUNCATION

In our approach, the cutoff of the front tail of the initial packet is the price we pay to obtain explicit analytic solutions. However, as we shall show in this section, this condition is not so restrictive. In fact, in most cases the effect of this truncation is so small that the probability densities of CWP's and EWP's become indistinguishable.

In this section, explicit analytic solutions will be derived, not only for the free case but also for situations involving potentials. Three simple cases will be considered, the free propagation case, the dispersion of the packets by a delta potential, and thin potential barriers in the low-energy regime.

The first step in our study is to analyze the effect of the truncation on the CWP's for $t>0$. In order to perform this task, we shall calculate and compare the time-dependent probability density $|\psi(x,t)|^2$ of CWP's and EWP's.

A. Free propagation case

We start our study by comparing the evolution of CWP's and EWP's for the simplest case of free propagation. Although the analytical solution for free EWP is well-known, and given by

$$\psi_0(x,t)=\frac{1}{(2\pi)^{1/4}}\frac{1}{\sigma^{1/2}}\frac{e^{i(k_0x-\hbar k^2t/2m)}}{\sqrt{1+i\dfrac{\hbar t}{2m\sigma^2}}}\times\exp\left\{-\frac{[x-x_0-\hbar kt/m]^2}{4\sigma^2\left[1+i\dfrac{\hbar t}{2m\sigma^2}\right]}\right\}, \tag{7}$$

we use it as reference point to test the consistency of our approach of CWP's, and to establish the basis to deal with more complex situations involving potentials.

In what follows we shall derive an exact analytic solution for the time evolution of the CWP's. Feeding the well-known free particle propagator,

$$K_f(x,t;y,0)=\sqrt{\frac{m}{2\pi\hbar t}}e^{im(x-y)^2/2\hbar t} \tag{8}$$

into Eq. (14) of Ref. [16], and using the identity [17]

$$\int_0^{\infty}dt\, e^{-(at^2+2bt+c)}=\frac{1}{2}\sqrt{\frac{\pi}{a}}e^{(b^2-ac)/a}\,\mathrm{erfc}\left[\frac{b}{\sqrt{a}}\right], \tag{9}$$

we obtain the following solution:

$$\psi_0^e(x,t)=\frac{1}{\sigma^{1/2}}\left(\frac{2}{\pi}\right)^{1/4}\frac{e^{imx^2/2\hbar t}}{\sqrt{1+i\dfrac{t}{\tau}}}\frac{w(iz_f)}{\sqrt{w(iz_0)}}, \tag{10}$$

with $\tau=(2m\sigma^2/\hbar)$, and z_f defined as

$$z_f=-\frac{i}{2}\sqrt{\frac{it}{2\tau}}\left[\frac{x/\sigma+it(ik_0\sigma+x_0/2\sigma)/\tau}{\sqrt{1+it/\tau}}\right]. \tag{11}$$

There are routines that can be used to easily evaluate the complex error function w appearing in Eq. (10). For example, using the method given in Ref. [19].

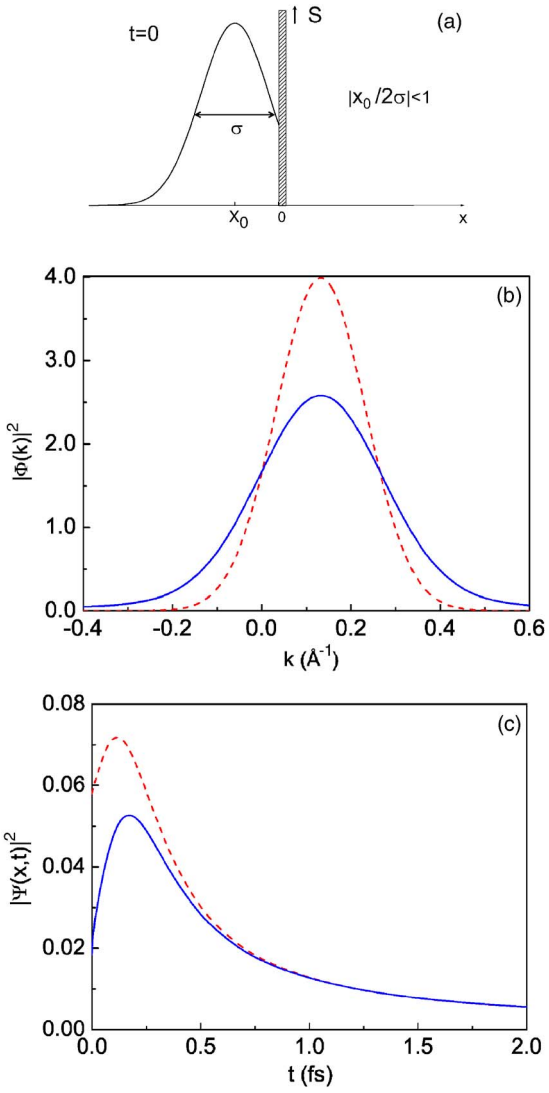

FIG. 2. (Color online) (a) Free Gaussian CWP with strong truncation ($|x_0/2\sigma|<1$) at $t=0$. Parameters: $x_0=-4.0$ Å, $\sigma=5.0$ Å, and $E_0=1.0$ eV. (b) Probability density in k space for the CWP (solid blue line) compared to the EWP (dashed red line). (c) Time evolution of the CWP at $x=0$, calculated from (10) (solid blue line), and compared to the EWP (dashed red line) calculated from Eq. (7).

An equivalent representation can also be obtained by setting $T(k)=1$ in Eq. (6), and integrating with respect to the variable k, that is,

$$\psi_0^e(x,t) = \Lambda_0 \int_{-\infty}^{\infty} dk\, w(iz) e^{ikx - i\hbar k^2 t/2m}. \tag{12}$$

Equations (10) and (12) are equivalent, and the latter will be used later in the following subsections.

We illustrate in Fig. 2(a) the quantum shutter model for a free Gaussian CWP with a strong truncation. In this case the parameters (given in the figure) are such that the relation $|x_0/2\sigma|<1$ is fulfilled, and hence the right tail of the initial packet is almost entirely cut off at $x=0$. In all of our calculations we shall use the effective mass, $m=0.067m_e$, where m_e is the electron mass.

The effect of the truncation of the probability density in k space is shown in Fig. 2(b). Here we plot the $|\Phi(k)|^2$ vs k, at $t=0$, for the CWP (solid blue line) calculated from Eq. (3). This is compared to the calculation of the probability density in k space for the EWP (dashed red line) given by the Fourier transform of Eq. (7) at $t=0$, and we note that the packet corresponding to the CWP is wider than the EWP in this space. The above is expected from the uncertainty principle as CWP is narrower than the EWP in x space (the former is extended just in the semispace $x<0$).

In Fig. 2(c) we compare the probability density $|\Psi(x,t)|^2$ as a function of time t and fixed position $x=0$ for both the CWP and EWP. Although roughly similar in shape, the curves exhibit differences in height as a consequence of the truncation of the initial wavepacket in the CWP case.

However, all the differences between the CWP's and EWP's observed in the previous figure rapidly disappear when the ratio $|x_0/2\sigma|$ is increased. Moreover, we can use the mathematical properties of the $w(z)$ function in this regime, to obtain an analytical expression for the solution more easy-to-use and even simpler than Eq. (10), provided that the condition $|x_0/2\sigma|>1$ is fulfilled. Notice that this condition is not so demanding, since it is sufficient that the distance $|x_0|$ of the initial packet to the shutter is about twice the width σ or larger.

In order to obtain the approximate analytical expression mentioned above, let us first consider the following properties of the $w(z)$ function. For very large values of the argument z, i.e., $|z|\gg 1$, the $w(iz)$ has the following series representation [14]:

$$w(iz) \simeq 2e^{z^2} + \frac{1}{\pi^{1/2} z} - \frac{1}{2\pi^{1/2} z^3} + \cdots, \tag{13}$$

provided that the phase ϕ_z of z lies in the interval $\pi/2<\phi_z<3\pi/2$. In the case of the free wavepacket given by Eq. (12), it is easy to convince oneself by inspection of Eq. (5) that the argument z always satisfy the above inequality since $\mathrm{Re}(z)<0$. Moreover, from Eq. (12) we can see that the argument z has in general a large value in the range of the k integration. However, in view of the fact that the main contributions of the integral arise from values of k in the vicinity of k_0, one may consider from Eq. (5) that $z\simeq(x/2\sigma)+i\Delta$ (where $\Delta\to 0$). Therefore, in order to use the properties of $w(z)$ given by Eq. (13), one has to guarantee that the condition $|z|\simeq|x/2\sigma|\gg 1$ is always satisfied; this is our condition for the small truncation regime. With these conditions fulfilled, one can approximate

$$w(iz) \simeq 2e^{z^2}. \tag{14}$$

By feeding the above approximation in Eq. (12), we obtain the following expression for the free CWP:

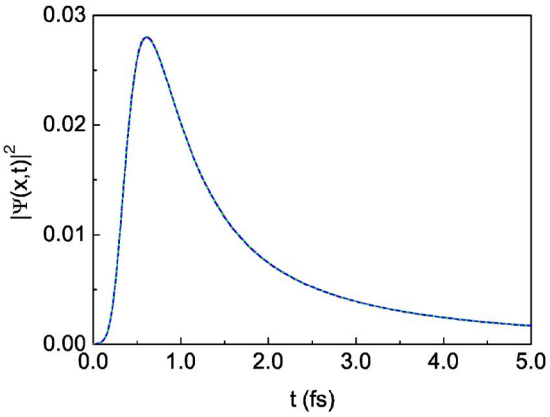

FIG. 3. (Color online) (a) Time evolution of $|\psi_\delta^e|^2$ for the delta potential at a fixed value of the position $x=0$, given by the integral representation Eq. (17) (solid blue line). Parameters: $x_0=-20.0$ Å, $\sigma=5.0$ Å, and $E_0=1.0$ eV, $\lambda=2.0$ eV Å. The calculations using the solution for an EWP [Eq. (19) from Ref. [4]] (dashed red line), and the analytical solution (19) (dotted green line), are included for comparison. All curves overlap.

$$\psi_0^{\mathrm{app}}(x,t)=\frac{1}{(2\pi)^{1/4}}\frac{1}{\sigma^{1/2}}\frac{e^{i(k_0x-\omega_0t)}}{\sqrt{1+i\dfrac{t}{\tau}}}\times\exp\left\{-\frac{[x-x_0-v_0t]^2}{4\sigma^2\left[1+i\dfrac{t}{\tau}\right]}\right\},\tag{15}$$

where we have defined the frequency $\omega_0=(E_0/\hbar)$, and the velocity $v_0=(\hbar k_0/m)$. Note that our free approximated solution, Eq. (15), is exactly the same as the free solution for EWP's, Eq. (7). This is an important test that confirms our initial assumption that our approach can accurately describe the evolution of EWP's in the small truncation regime. In what follows we shall apply this idea to the more complex situations involving potentials.

B. Delta potential barrier case

The transmission amplitude for a delta potential $V(x)=\lambda\delta(x)$ is given by

$$T(k)=\frac{k}{k+i(m\lambda/\hbar^2)}.\tag{16}$$

Using this expression for $T(k)$ in the formal solution, Eq. (6), we obtain after simple algebra, the dynamical solution for CWP's incident on a delta potential barrier; it reads

$$\psi_\delta^e(x,t)=\psi_0^e(x,t)-\Lambda_\lambda\int_{-\infty}^{\infty}\frac{dk\,w(iz)e^{ikx}e^{-i\hbar k^2t/2m}}{k+i(m\lambda/\hbar^2)},\tag{17}$$

where we have defined the parameter $\Lambda_\lambda\equiv(im\lambda/\hbar^2)\Lambda_0$. From the above expression it is easy to see that the free solution $\psi_0^e(x,t)$ is naturally recovered in the limit $\lambda\to0$.

Calculations of the time-dependent probability density are depicted in Fig. 3, where we show a plot of $|\Psi(x,t)|^2$ vs t at the fixed position $x=0$ for the CWP incident on a delta potential (solid blue line). The parameters are given in the figure. This is compared to the calculation of the probability density corresponding to the EWP with the same parameters (dashed red line). The latter was done evaluating numerically the integral solution obtained by Elberfeld and Kleber [4]. Both calculations coincide almost perfectly, implying that the CWP's are excellent approximations for EWP's, even in the presence of a potential, with the unique condition that we are in the small truncation regime.

This equivalence is relevant since we can derive analytical solutions for wavepackets that otherwise can only be numerically treated. This can be done by exploiting the mathematical properties of the complex error functions involved in the exact solutions (12) and (17).

For wavepackets with a small cutoff, i.e., $|x_0/2\sigma|>1$, we can, as in the free case, use the approximation (14) in the integral representations given by Eqs. (12) and (17), and using the identity

$$M(x';q';t')=\frac{i}{2\pi}\int_{-\infty}^{\infty}dk\frac{e^{ikx'}e^{-i\hbar k^2t'/2m}}{k-q'},\tag{18}$$

to obtain an approximate analytical solution for the delta potential case. This solution reads

$$\psi_\delta^{\mathrm{app}}=\psi_0^{\mathrm{app}}(x,t)-\frac{1}{(2\pi)^{1/4}}\frac{1}{\sigma^{1/2}}e^{i(k_0x-\omega_0t)}\times\sqrt{\pi}(2m\sigma\lambda/\hbar^2)M(x'';q'';t''),\tag{19}$$

where we have defined

$$x''=x-x_0-v_0t,$$

$$q''=-(k_0+im\lambda/\hbar^2),$$

$$t''=t-i\tau.\tag{20}$$

The quantities $M(x';q';t')$ are known as Moshinsky functions [14,20], and are defined by

$$M(y')=\frac{1}{2}e^{imx'^2/2\hbar t'}w(iy'),\tag{21}$$

where the argument y' of the complex error function $w(iy')$ is given by,

$$y'=e^{-i\pi/4}\sqrt{\frac{m}{2\hbar t'}}\left[x'-\frac{\hbar q'}{m}t'\right].\tag{22}$$

The new expression for the time-dependent solution, Eq. (19), is analytical and simpler than (17), where we just need to evaluate the Moshinsky function instead of performing the time-consuming numerical integration required to evaluate (17). In Fig. 3 we have included the calculation of $|\Psi(x,t)|^2$ vs t at $x=0$ using this approximate expression for the solution (dotted green line). All curves overlap illustrating that the description of Eq. (19) is excellent. It is important to stress that Eq. (19) not only reproduces the calculations of the exact integral solution, Eq. (17), but also the numerical solution of the Gaussian EWP, widely used in the study of

time-dependent tunneling problems [4]. Therefore the analytic expression for the solution, Eq. (19), can also describe EWP's in the considered regime.

C. The finite barrier case

Let us consider a rectangular potential barrier of height V_0 and width L, defined along the region, $0 \leqslant x \leqslant L$. The potential barrier systems can also be characterized in terms of the opacity α, defined as $\alpha=(k_{V_0}L)$, with $k_{V_0}=[2mV_0]^{1/2}/\hbar$. The transmission amplitude $T(k)$ is given by

$$T(k) = \left[\cosh(\kappa L) - i\frac{k^2-\kappa^2}{2k\kappa}\sinh(\kappa L)\right]^{-1} e^{-ikL}, \quad (23)$$

where we have defined $\kappa^2=(k_{V_0}^2-k^2)$. In the low-energy regime ($k \ll k_{V_0}$), we have that $\kappa \to k_{V_0}=(\alpha/L)$, which allows to approximate Eq. (23) by

$$T(k) \simeq \left[\cosh\alpha + i\frac{\alpha}{2kL}\sinh\alpha\right]^{-1} e^{-ikL}. \quad (24)$$

For the case of potential barriers with small opacities ($\alpha \ll 1$), we can make the approximations $\cosh\alpha \simeq 1$, and $\sinh\alpha \simeq \alpha$, which allows us to write

$$T(k) \simeq \left[1 + i\frac{\alpha^2}{2kL}\right]^{-1} e^{-ikL} = \frac{ke^{-ikL}}{k + i(mV_0L/\hbar^2)}. \quad (25)$$

In order to obtain the time-dependent solution for this case, we proceed as follows. First we feed into our formal solution, Eq. (6), the obtained transmission amplitude, Eq. (25), and the approximate w function, Eq. (14). Using Eq. (18), and with the help of the Gaussian integral,

$$\int_{-\infty}^{\infty} dy\, e^{-uy^2} e^{-vy} = \sqrt{\frac{\pi}{u}} e^{-v^2/4u}, \quad (26)$$

we obtain the solution

$$\psi_b^{\text{app}} = \psi_0^{\text{app}}(x-L,t) - \frac{1}{(2\pi)^{1/4}}\frac{1}{\sigma^{1/2}} e^{i[k_0(x-L)-\omega_0 t]} \times \sqrt{\pi}(2m\sigma V_0 L/\hbar^2) M(x_b;q_b;t_b), \quad (27)$$

where we have defined,

$$x_b = x - L - x_0 - v_0 t,$$

$$q_b = -(k_0 + i\alpha^2/2L),$$

$$t_b = t - i\tau. \quad (28)$$

The above solution is very similar to the delta potential case, given by Eq. (19). Actually, Eq. (27) can be obtained directly from the delta case solution (19), by letting $\lambda = V_0 L$, and performing the translation $x \to (x-L)$.

Let us consider in Fig. 4 the time evolution of $|\psi_b^{\text{app}}|^2$ (solid red line), measured at the barrier edge $x=L$, with potential parameters $V_0=0.1$ eV and $L=2.5$ Å. The initial CWP is centered at $x_0=-50.0$ Å, with $\sigma=5.0$ Å, and an incidence energy $E_0=1.0\times10^{-3}$ eV. Here we have included for comparison a plot of the probability density (dashed black line), using Eq. (6) with the exact transmission amplitude given by Eq. (23). As can be appreciated from the figure, they agree very well showing that the analytical solution is a good approximation to the numerical one.

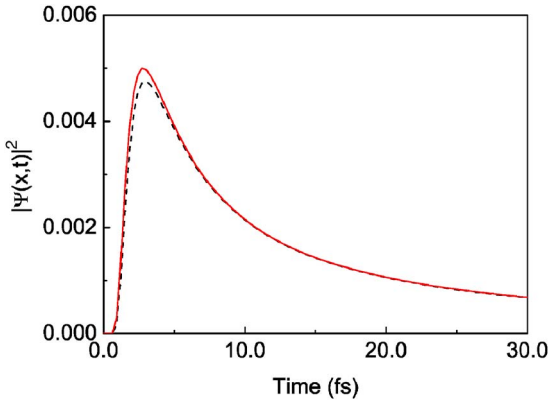

FIG. 4. (Color online) Time evolution of $|\psi_b^{\text{app}}|^2$ (solid red line) for a thin potential barrier ($\alpha=0.1047$), in the low-energy regime, measured at $x=L$. The potential parameters are $V_0=0.1$ eV, and $L=2.5$ Å; the CWP parameters are $x_0=-50.0$ Å, $\sigma=5.0$ Å, with an incidence energy $E_0=1.0\times10^{-3}$ eV. For comparison, we included a plot of the probability density (dashed black line), using Eq. (6) with the exact transmission amplitude given by Eq. (23).

At this point it is important to emphasize the generality of the solution Eq. (6) and the possibility to derive analytical solutions for more complex structures. As illustrated here for the potential barrier case, all we need is a suitable expression for the transmission amplitude $T(k)$. For example, in systems involving resonances such as double barriers or superlattices, Breit-Wigner-type expressions for $T(k)$ could be used.

IV. ANALYSIS OF THE DELAY TIME

With the new tools developed so far, we are ready to perform a systematical study of the delay time, and extend the study to unexplored regions. Before performing this task, let us explore a useful rescaling property of the solutions.

In order to exemplify the above, let us consider the time evolution of $|\psi_\delta^{\text{app}}|^2$ for two different systems called A and B. System A is the one considered in Fig. 3, that is, the system with parameters $x_0=-20.0$ Å, $\sigma=5.0$ Å, $E_0=1.0$ eV ($k_0=0.1325$ Å^{-1}), and $\lambda=2.0$ eV Å. System B has parameters $x_0=-40.0$ Å, $\sigma=10.0$ Å, $E_0=0.25$ eV ($k_0=0.06626$ Å^{-1}), and $\lambda=1.0$ eV Å. In Fig. 5(a) we plot their corresponding time-dependent probability densities. However, if we now consider the probability densities of systems A and B in such a way that we now plot $\sigma|\psi_\delta^{\text{app}}|^2$ vs (t/τ), we find that both curves coincide perfectly. This invariance under rescaling is illustrated in 5(b), where the plots are now indistinguishable among them. This coincidence arises from the fact that we have (intentionally) chosen the parameters so that the dimensionless quantities $k_0\sigma$ and (x_0/σ) are the same for both systems. This is evidence of an underlying rescaling property of the solutions.

The rescaling property illustrated in the above numerical example, is in fact a general feature of our solutions. We

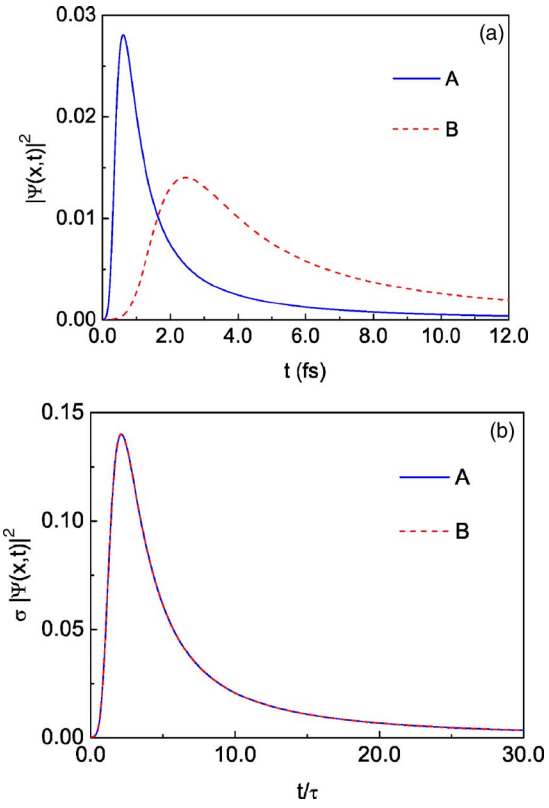

FIG. 5. (Color online) (a) Probability density at $x=0$ for the delta potential case using the analytical solution given by Eq. (19) for systems A (solid blue line), and B (dashed red line). (b) Rescaled probability density $\sigma|\psi_\delta^{\text{app}}|^2$ as a function (t/τ) for the systems depicted in (a). The curves of systems A and B are indistinguishable among them.

have found that the solutions for the different cases considered so far, Eqs. (6), (10), (12), (15), (17), (19), and (27) can all be rescaled in this special manner. See the Appendix. In this way, a rescaled solution, instead of representing a given system, will represent a set of systems that share similar characteristics. We will take advantage of this property in our study of the delay time, exploring a large number of systems in a single calculation.

The rescaled delay time T_D is calculated by measuring the time differences of the maxima of the probability densities of the free and delta cases. The dynamical time scale is then given by

$$T_D = T_\delta^{\text{app}} - T_0^{\text{app}}, \tag{29}$$

where T_0^{app} is obtained from the maximum of $|\Psi_0^{\text{app}}(X,T)|^2$ calculated from the rescaled free solution ((A15)), and T_δ^{app} from the maximum of $|\Psi_\delta^{\text{app}}(X,T)|^2$ evaluated using the rescaled solution of the delta potential (A16). Notice that T_D is evaluated in the rescaled coordinates (X,T), defined in the Appendix, and according to Eq. (A7), T_D is a dimensionless quantity.

We shall analyze the behavior of T_D as function of two parameters: K_0, β, at fixed values of X_0 and $X=0$. All the systems with the same pair (K_0,β) will have exactly the same behavior; in this sense each pair (K_0,β) represents a family of similar systems.

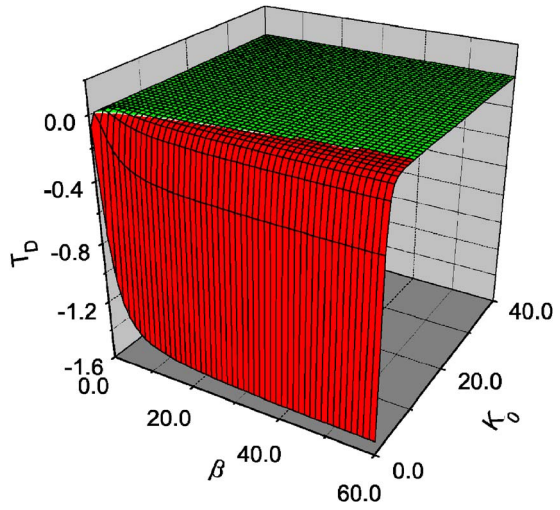

FIG. 6. (Color online) Delay time T_D at $X=0$ for a CWP initially centered at $X_0=-4.0$. An apparently flat region of negligible $T_D>0$ [green (top) surface] appears for a wide range of values of the rescaled parameters K_0 and β. A region of $T_D<0$ [red (front) surface] is also appreciated, and is related to a filtering process. See text.

We present in Fig. 6 the calculation of T_D as a function of the parameters K_0 and β, for the case $X_0=-4.0$. We notice a regime (red region) for small values of K_0 (roughly $K_0 \leqslant 10.0$ in this calculation), where the time differences of peaks, given by Eq. (29), yield $T_D<0$. This effect must be related to a filtering process as discussed in Ref. [21]. The delta is acting as a filter of high-energy components of the wavepacket, and therefore the peak of the transmitted packet T_δ^{app} appears earlier than its free counterpart T_0^{app}. See also Ref. [8]. Moreover, a region of delay time is clearly appreciated (green region) as a large plateau in the surface in Fig. 6. As we shall show below this region is not so flat at all, and exhibits structure when viewed at an appropriate scale. In Fig. 7(a) we illustrate this in detail by plotting an amplification of the plateau of Fig. 6, and a hump is clearly appreciated. This special structure is related with the antibound state of the delta potential, $K_{ab}=-i\beta/2$, as it will be clarified after we compare our dynamical delay time with the well-known expression for the phase time [22]. As discussed in Ref. [23] the phase time can be computed as an energy derivative of the phase of the transmission amplitude. For the case of the delta potential, the phase time can be obtained by using Eq. (16), which yields

$$t_\phi = \left(\frac{m}{\hbar k_0}\right)\frac{(m\lambda/\hbar^2)}{(m\lambda/\hbar^2)^2 + k_0^2}. \tag{30}$$

The rescaled phase time $T_\phi=(t_\phi/\tau)$ is given by

$$T_\phi = \frac{(\beta/K_0)}{\beta^2 + 4K_0^2}. \tag{31}$$

In Fig. 7(b) we calculate the phase time for the delta potential T_ϕ using the same parameters as in Fig. 7(a). Note

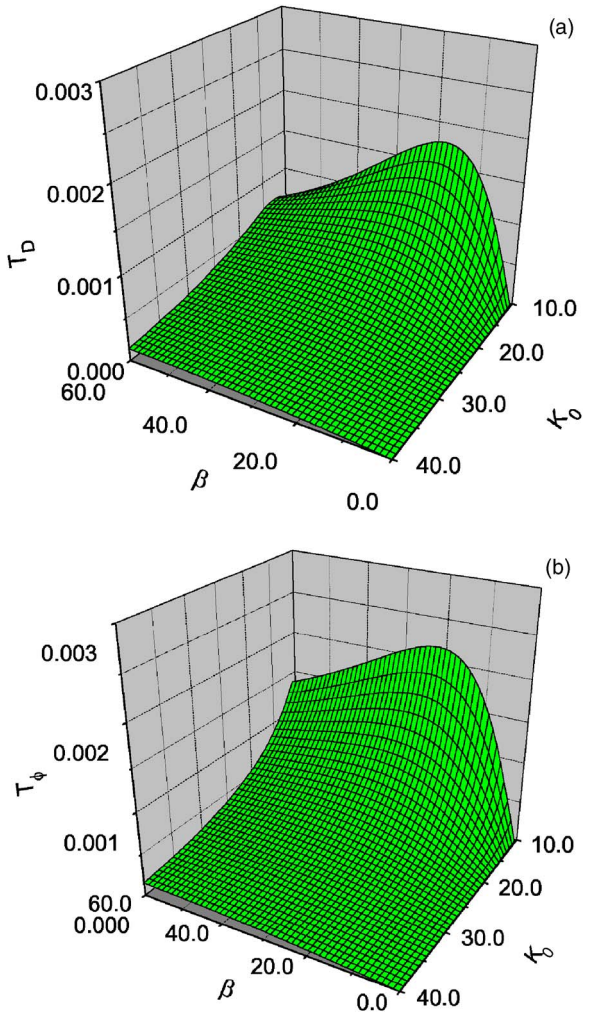

FIG. 7. (Color online) (a) Amplification of the plateau of the surface presented in the previous figure that shows delay time in more detail. (b) The surface corresponding to the rescaled exact phase time T_ϕ is included for comparison with (a).

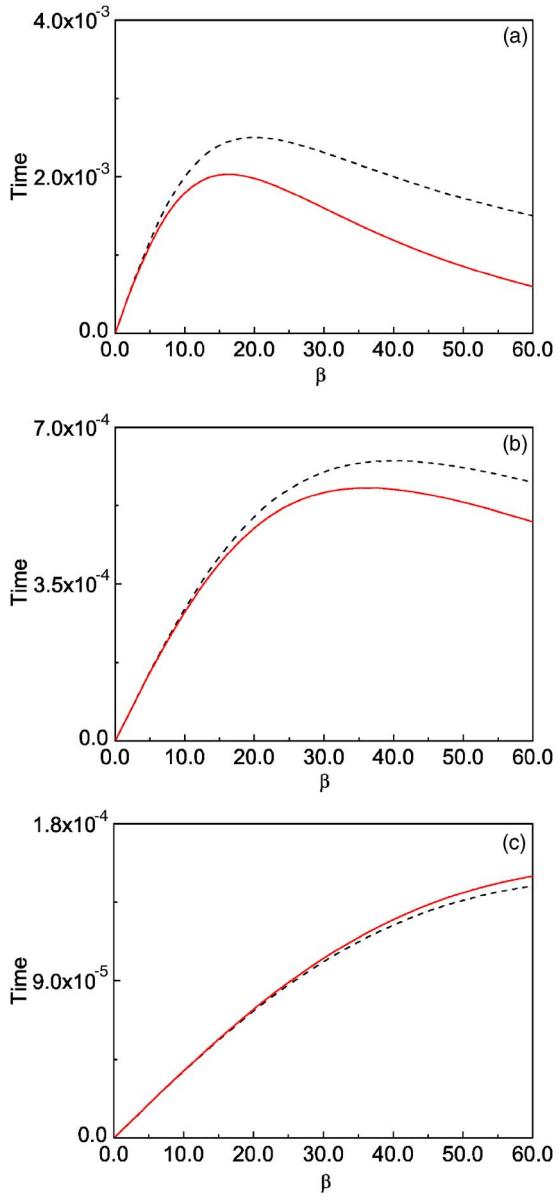

FIG. 8. (Color online) Delay time T_D (red solid line) and phase time T_ϕ (black dashed line) at $X=0$ as a function of β for different values of the dimensionless momentum K_0: (a) $K_0=10.0$, (b) $K_0=20.0$, and (c) $K_0=40.0$. The initial position of the CWP in the rescaled coordinates is $X_0=-4.0$.

that both surfaces in 7(a) and 7(b), although not exactly the same, exhibit similar structure. Sections of both surfaces are shown in Fig. 8 for representative values of K_0. Notice the perfect agreement between T_D and T_ϕ for small values of β. This occurs roughly for values of $\beta \leqslant K_0$, as can be seen by visual inspection of Fig. 8.

It can be easily shown from Eq. (31), that the maximum exhibited by the phase time in the graphs occurs exactly at $K_0=(\beta/2)=|K_{ab}|$, i.e., the magnitude of the antibound state of the delta potential. In view of the similarities of T_D and T_ϕ exhibited in Figs. 7 and 8, it is clear that the antibound state is also responsible for the maximum of our dynamical delay time. The importance of the antibound state on both the phase time and the delay time was noticed earlier by Hernández and García-Calderón [6] in the problem of tunneling of cutoff plane waves in a delta potential.

V. CONCLUDING REMARKS

A formal solution for tunneling Gaussian wavepackets was derived exactly within the framework of the quantum shutter approach. The general solution, valid for finite-range potentials of arbitrary shape, was applied to particular systems of interest, and simple analytic expression for their corresponding wave functions were derived. We showed that the solutions satisfy a useful rescaling property that was applied here to study the delay time. This interesting mathematical property allowed us to explore this time scale for a wide range of parameters.

The main results of our study of the delay time can be summarized as follows. (i) Our dynamical time scale T_D was analyzed in terms of two special rescaled parameters: K_0 and β. The former is related to the momentum, and the latter to the intensity of the delta potential. For small values of K_0, a strong filtering effect of high-energy components of the

wavepacket dominated the process, whereas for larger values of K_0, a region of negligible time delay is observed (this holds for a wide range of values of β). (ii) The phase time was also calculated in terms of the parameters K_0 and β and compared with our dynamical time delay. An excellent agreement was obtained for small values of β, implying that the phase time, which is a stationary time scale, works well in the vicinity of the interaction region ($X=0$). This is important to emphasize since this is not the case for other kind of initial conditions, such as cutoff plane waves, as shown recently by Hernández and García-Calderón [6].

The analysis of the effect of truncation of the initial state on the evolution of the probability density is also one of the important contributions of the present work. We found a regime ($|x_0/2\sigma|>1$) in which the analytic solutions of the CWP's perfectly coincide with the calculations of the EWP's. This means that the analytic solutions of the CWP's can also be used as practical and fast computational tools for the EWP's in that regime.

As a final remark, the formal solution (6) is valid for potentials of arbitrary shape, and the only input is the transmission amplitude $T(E)$, which, for more complex systems such as superlattices, can be calculated using transfer matrix. It is important to emphasize, however, that this solution is valid only for the transmission region $x>L$. The solution for the internal region ($0\leqslant x\leqslant L$) requires the use of a different propagator.

ACKNOWLEDGMENTS

We acknowledge financial support from 8VA, and 10MA Convocatoria Interna-UABC. J.V. also acknowledges financial support from El Ministerio de Educación y Ciencia, Spain, under Grant No. SB2005-0047.

APPENDIX: RESCALING OF THE SOLUTIONS

The regularities observed in our formulas for the probability density arise from a simple rescaling property of Schrödinger's equation and the corresponding initial condition. By feeding the dimensionless variable $X=(x/\sigma)$ into the time-independent Schrödinger equation for the delta potential,

$$\left[-\frac{\partial^2}{\partial x^2}+\frac{2m}{\hbar^2}\lambda\delta(x)-k_0^2\right]\psi(x)=0, \tag{A1}$$

we obtain,

$$\left[-\frac{\partial^2}{\partial X^2}+\frac{2m}{\hbar^2}\sigma\lambda\delta(X)-(k_0\sigma)^2\right]\psi(X)=0. \tag{A2}$$

In the above equation we can identify the dimensionless parameters for the momentum $K_0=k_0\sigma$ and the effective potential $\beta=(2m\sigma\lambda/\hbar^2)$. This allows us to write the rescaled Schrödinger's equation as

$$\left[-\frac{\partial^2}{\partial X^2}+\beta\delta(X)-K_0^2\right]\psi(X)=0. \tag{A3}$$

By performing the above rescaling for the time-dependent Schrödinger's equation,

$$\left[-\frac{\partial^2}{\partial x^2}+\frac{\hbar^2}{2m}\lambda\delta(x)-i\frac{2m}{\hbar}\frac{\partial}{\partial t}\right]\psi(x,t)=0, \tag{A4}$$

we obtain

$$\left[-\frac{\partial^2}{\partial X^2}+\beta\delta(X)-i\frac{\partial}{\partial T}\right]\psi(X,T)=0, \tag{A5}$$

where the dimensionless variable of time is defined as $T=(t/\tau)$. Similarly, the Gaussian CWP initial condition given by Eq. (1) becomes

$$\psi(X,T=0)=\begin{cases}A' e^{-(X-X_0)^2/4}e^{iK_0X}, & -\infty<X\leqslant 0,\\ 0, & X>0.\end{cases} \tag{A6}$$

with $X_0=(x_0/\sigma)$ and $\psi(X,T)$ as the rescaled time dependent-solution. It is clear that $\psi(X,T)$ only depends on the parameters β, X_0, and K_0. That is, for a fixed value of X_0, all the systems with the same parameter K_0 and β yield the same $\psi(X,T)$.

The above results allow us to rescale all of our formulas considered so far, by using the set of dimensionless variables

$$X=x/\sigma,$$

$$X_0=x_0/\sigma,$$

$$T=t/\tau,$$

$$K=k\sigma,$$

$$K_0=k_0\sigma,$$

$$\beta=2m\sigma\lambda/\hbar^2. \tag{A7}$$

With these new rescaled variables, the general solution given by Eq. (6) can be rewritten as

$$\Psi(X,T)=\sqrt{\sigma}\psi(x,t)=\Lambda'\int_{-\infty}^{\infty}dK\, w(iZ)T(K)e^{iKX-iK^2T}, \tag{A8}$$

with the definitions

$$\Lambda'=\frac{1}{2\pi}\sqrt{\frac{1}{\sqrt{2}\pi}}\frac{1}{\sqrt{w(iZ_0)}},$$

$$Z_0=X_0/\sqrt{2},$$

$$Z=X_0/2+i(K_0-K), \tag{A9}$$

where Λ' is related to the normalization constant A'.

For the particular case of the free Gaussian wavepacket, the rescaled version of the integral solution, Eq. (12), reads

$$\Psi_0(X,T) = \sqrt{\sigma}\psi_0(x,t) = \Lambda' \int_{-\infty}^{\infty} dK\, w(iZ) e^{iKX - iK^2 T}. \tag{A10}$$

Similarly, the rescaled exact solution for the free particle case reads

$$\Psi_0^e(X,T) = \sqrt{\sigma}\psi_0^e = \left(\frac{2}{\pi}\right)^{1/4} \frac{e^{iX^2/4T}}{\sqrt{1+iT}} \frac{w(iZ_f)}{\sqrt{w(iZ_0)}}, \tag{A11}$$

with

$$Z_f = -i\frac{1}{T}\left[\frac{X + i(iK_0 + X_0/2)/T}{\sqrt{1 - i/T}}\right]. \tag{A12}$$

That is, Eq. (A11) is the rescaled version of the solution given by (10).

For the particular case of the delta potential, the rescaled transmission amplitude reads

$$T(K) = \frac{K}{K + i\beta/2} \tag{A13}$$

and the rescaled integral representation of the solution (17) is written as

$$\Psi_\delta^e(X,T) = \sqrt{\sigma}\psi_\delta^e(x,t) = \Lambda' \int_{-\infty}^{\infty} dK\, w(iZ) T(K) e^{iKX - iK^2 T}. \tag{A14}$$

We also perform the rescaling procedure for the solutions corresponding to the small cutoff regime $|X_0/2| > 1$. For the free propagation case we have

$$\Psi_0^{\text{app}}(X,T) = \sqrt{\sigma}\psi_0^{\text{app}} = \frac{1}{(2\pi)^{1/4}} \frac{e^{i(K_0 X - K_0^2 T)}}{\sqrt{1+iT}} \times \exp\left\{-\frac{[X - X_0 - 2K_0 T]^2}{4[1+iT]}\right\}, \tag{A15}$$

and for the rescaled delta potential case we have $\Psi_\delta^{\text{app}}(X,T) = \sigma^{1/2}\psi_\delta^{\text{app}}$, given by

$$\Psi_\delta^{\text{app}}(X,T) = \Psi_0^{\text{app}}(X,T) - \frac{1}{(2\pi)^{1/4}} e^{i(K_0 X - K_0^2 T)} \times \sqrt{\pi}\beta M(X'';Q'';T''), \tag{A16}$$

where we have defined

$$X'' = X - X_0 - 2K_0 T,$$

$$Q'' = -(K_0 + i\beta/2),$$

$$T'' = 2m(T-i)/\hbar. \tag{A17}$$

For the case of the potential barrier in the low-energy regime, and small values of the opacity ($\alpha \ll 1$), we have $\Psi_b^{\text{app}}(X,T) = \sigma^{1/2}\psi_b^{\text{app}}$, given by

$$\Psi_b^{\text{app}}(X,T) = \Psi_0^{\text{app}}(X - L_\sigma, T) - \frac{1}{(2\pi)^{1/4}} e^{i[K_0(X - L_\sigma) - K_0^2 T]} \times \sqrt{\pi}\left[\frac{\alpha^2}{L_\sigma}\right] M(X_b'';Q_b'';T_b''), \tag{A18}$$

with

$$L_\sigma = L/\sigma,$$

$$X_b'' = X - L_\sigma - X_0 - 2K_0 T,$$

$$Q_b'' = -(K_0 + i\alpha^2/2L_\sigma),$$

$$T_b'' = 2m(T-i)/\hbar. \tag{A19}$$

Equations (A15), (A16), and (A18) are the rescaling of Eqs. (15), (19), and (27), respectively.

[1] L. A. MacColl, Phys. Rev. **40**, 621 (1932).
[2] T. E. Hartman, J. Appl. Phys. **33**, 3427 (1962).
[3] H. M. S. A. Goldberg and J. L. Schwartz, Am. J. Phys. **35**, 117 (1967).
[4] W. Elberfeld and M. Kleber, Am. J. Phys. **56**, 155 (1988).
[5] J. A. Støvneng and E. H. Hauge, Phys. Rev. B **44**, 13582 (1991).
[6] A. Hernández and G. García-Calderón, Phys. Rev. A **68**, 014104 (2003).
[7] H. P. Simanjuntak and P. Pereyra, Phys. Rev. B **67**, 045301 (2003).
[8] S. L. Konsek and T. P. Pearsall, Phys. Rev. B **67**, 045306 (2003).
[9] S. B. A. L. Pérez Prieto and J. G. Muga, J. Phys. A **36**, 2371 (2003).
[10] M. A. Andreata and V. Dodonov, J. Phys. A **37**, 2423 (2004).
[11] Y. Fu and M. Willander, J. Appl. Phys. **97**, 094311 (2005).
[12] E. Granot and A. Marchewka, Europhys. Lett. **72**, 341 (2005).
[13] N. Yamada, G. García-Calderón, and J. Villavicencio, Phys. Rev. A **72**, 012106 (2005).
[14] G. García-Calderón and A. Rubio, Phys. Rev. A **55**, 3361 (1997).
[15] G. García-Calderón and J. Villavicencio, Phys. Rev. A **64**, 012107 (2001).
[16] G. García-Calderón, J. Villavicencio, and N. Yamada, Phys. Rev. A **67**, 052106 (2003).
[17] *Handbook of Mathematical Functions*, edited by M. Abramowitz and I. A. Stegun (Dover, New York, 1964), p. 297.
[18] V. N. Faddeyeva and N. M. Terent'ev, in *Tables of Values of*

The Function $w(z)=e^{-z^2}\left(1+\frac{2i}{\sqrt{\pi}}\int_0^z e^{t^2}dt\right)$ *for Complex Argument*, edited by translated from the Russian by D. G. Fry and B. A. Hons (Pergamon, London, 1961).

[19] G. P. M. Poppe and C. M. J. Wijers, ACM Trans. Math. Softw. **16**, 38 (1990).

[20] M. Moshinsky, Phys. Rev. **88**, 625 (1952).

[21] R. Landauer and Th. Martin, Rev. Mod. Phys. **66**, 217 (1994).

[22] D. Bohm, *Quantum Theory* (Prentice-Hall, New York, 1954).

[23] J. Villavicencio and G. García-Calderón, Phys. Rev. A **70**, 032107 (2004).